ISSN 1392 - 1207. MECHANIKA. 2011. 17(6): 674-680

Simulation of different forming mode of wire based on thermo-mechanical coupling method

Licheng Yang*, Jingxiang Hu*, Liwei Ning*, A. Romagos**
**Department of Mechanical Engineering, Hunan Institute of Engineering, Xiangtan 411104, China, E-mail: ylich2008@163.com*
***Faculty of Engineering, University of Technology, Sydney 2007, Australia*

crossref http://dx.doi.org/10.5755/j01.mech.17.6.1013

1. Introduction

The rolling process is mainly used to produce sectional iron, wire, rod, plate and tube or is widely used for manufacturing the semifinished products, finished products and metallic equipment. The hot rolling of wire is a major plastic forming way of material because the forming format has the characteristics of the grain refinement, eliminating the microstructure defect, densifying the structure and improving mechanical properties. For the hot rolling process, the large plastic deformation occurs in the rolling metal under the application of a series of rotating rollers, along with the complex heat transfer phenomena in the rolling process: thermal convection between the workpiece / rollers and the surrounding environment, thermal conduction between the workpiece and rollers, heat generation due to friction and plastic deformation, the descaling stage or forced water convection. Especially, the heat radiation belongs to nonlinear problem. The temperature variation of the workpiece has an important influence on structural deformation and material properties, moreover, the structural deformation also can change inversely thermal boundary conditions, which affects directly the distribution of the temperature. Thus, it shows there are interaction phenomena between temperature field and displacement field. The forming process involves in material, geometry and contact nonlinearities. Therefore, it is difficult to obtain analytical solutions for all kinds of mechanical and deformation parameters in the hot rolling process. For the rollers of different passes, the metal flow pattern is different in the rolling process, which causes different rolling deformation and mechanical properties. The accurate prediction of deformation and force in rolling process of different rollers is valuable for the adjustment and optimization of process parameters and improvement of product quality.

In the past decades, many researchers use a variety of analytical and numerical methods to study the rolling process, such as slip field method [1], upper bound method [2], finite difference method [3], boundary element method [4] and the finite element method (FEM) [5, 6], which is useful for discovering the forming property of the metal. The application of numerical method in the metal forming process becomes gradually to one of the frontiers of research areas. For example, Liu studied the rolling pressure distribution along strip width during the cold rolling process using 3D elastic-plastic FEM [7]. Kim presented an on-line model for the prediction of temperature distributions along the thickness of the strip in the finishing mill [8]. The thermal boundary conditions as well as heat generation due to deformation were discussed in their model. Zhang developed a three-dimensional model to study the plastic deformation of strip, thermal crown of rolls, roll deflection and flattening [9]. Richelsen used full three-dimensional numerical method to investigate the effect of the width spread in the rolling process [10]. In their model, the contact and friction between roll and plate were defined by interfacial constitutive relation, and the friction model was considered based on rolling direction and the transverse direction. Du corrected the stiffness of friction element by using the thickness of friction element and friction coefficient of contact surface in his model [11]. In fact, the precision of prediction results mainly depends on the correct contact definition between the workpiece and the rolls. The study of the contact problem has been rare in the relative literature in the past. Duan studied the distribution of contact pressure, equivalent strain, temperature, stress, rolling force and torque of the workpiece based on thermo-mechanical coupled FEM program FORGE3 [12]. Arif calculated pressure distribution and friction stress and studied Von Mises stress inside the roll at different radius [13]. Phaniraj utilized the commercial finite element software (DEFORM) to simulate temperature profiles and distribution of points of the strip surface and the strip center in hot rolling process when the workpiece traveled through the finishing mill [14]. Serajzadeh used rigid-viscoplastic FEM to predict the strain distributions within the rolled metal at different positions in the deformation zone and the effect of various process parameters, such as initial strip temperature, rolling speed, lubrication on the strain in the hot rolling process [15]. The previous research mainly discovered the stress distribution and deformation characteristics under the application of thermo-mechanical coupling.

The pass system for the wire/rod forming mainly includes two rollers per pass with alternate flat-box-oval-round type, Y type three round-flat rollers or Y type three arc-flat rollers. Y type three-roller mill is made up of three ring rollers with 120° layout, which causes the twist-free, microtension rolling state. Thus it can improve the product surface quality and yield of wire product. In the present paper, by considering various thermal boundary conditions, material properties and initial conditions, the mechanical properties, deformation mechanism and temperature distribution of the same round workpiece are studied in the three pass systems, such as two rollers of alternative oval-round passes, Y type three round-flat rollers and Y type three arc-flat rollers.

2. Mathematical model

2.1. Governing equations and boundary condition

To predict the temperature distribution of the workpiece in the hot continuous rolling process, it is necessary to derive the corresponding differential equations and boundary conditions of the rolls and workpiece. When the workpiece is in the rolling state, the governing heat exchange equation for the workpiece can be written as

$$\frac{\partial}{\partial x}\left(k\frac{\partial T}{\partial x}\right)+\frac{\partial}{\partial y}\left(k\frac{\partial T}{\partial y}\right)+\frac{\partial}{\partial z}\left(k\frac{\partial T}{\partial z}\right)+\dot{q}=\rho c\frac{\partial T}{\partial t} \quad (1)$$

where ρ is the workpiece density, T is temperature, c is the specific heat, k is the thermal conductivity, and $\dot{q}$ shows the volumetric rate of heat generation due to the plastic deformation.

It is obvious that the contact state of the roller is variable in hot rolling process, and the corresponding temperature distribution of the roller surface is changeable with the different contact state. It should consider to the solution of the governing equation of the rolls in order to predict accurately the temperature distribution of the workpiece. Similarly, the corresponding governing equation of the rollers is given as the following equation by using cylindrical coordinate system (r, θ, z).

$$\frac{1}{r}\frac{\partial}{\partial r}\left(k_r r\frac{\partial T}{\partial r}\right)+\frac{1}{r^2}\frac{\partial}{\partial \theta}\left(k_r\frac{\partial T}{\partial \theta}\right)+\frac{\partial}{\partial z}\left(k_r\frac{\partial T}{\partial z}\right)=\rho_r c_r\frac{\partial T}{\partial t} \quad (2)$$

where ρ_r is the roll density, and c_r is specific heat of the roller. In order to resolve the Eqs. (1) and (2), the boundary condition is shown in Fig. 1.

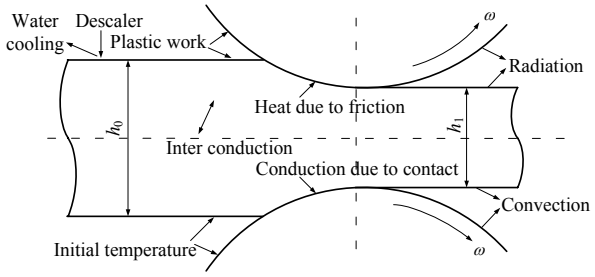

Fig. 1 Thermal exchange phenomena during hot rolling

As shown in Fig. 1, the thermal exchange phenomena during the hot rolling main include heat generation and the thermal exchange between the rollers and other bodies.

2.1.1. Heat generation

When the workpiece contacts with the rollers, it occurs large plastic deformation, which a great deal of heat is produced due to plastic deformation work. The heat generation of the workpiece due to plastic deformation can be expressed as

$$\dot{q}_{def}=\eta\bar{\sigma}\dot{\bar{\varepsilon}} \quad (3)$$

where $\dot{q}_{def}$ is heat generation rate due to plastic deformation, η is the efficiency of conversion of deformation energy to heat, $\bar{\sigma}$ and $\dot{\bar{\varepsilon}}$ are effective flow stress and equivalent strain rate, respectively. Moreover, friction work at the rollers-workpiece interface can also generate heat, thus it makes temperature change markedly in forward slip zone and backward slip zone. The distributed surface flux is generated from the frictional phenomenon

$$q_f=\tau_f A_c v_r \delta t \quad (4)$$

where q_f is heat generation due to friction work, A_c is the contact area, v_r is the relative slipping velocity along the arc length of contact, δt is time increment step, and the friction shear stress τ_f is expressed as

$$\tau_f=-m\frac{\bar{\sigma}}{\sqrt{3}}\frac{2}{\pi}arctan\left(\frac{v_r}{a}\right)\bar{\tau} \quad (5)$$

where m is friction factor and follows the law of constant friction, σ_0 is the yield stress, $\bar{\tau}$ shows frictional stress direction, a is a constant value and equals to the value of be 1% to 10% of a typical relative sliding velocity, v_r. Thus, the shear frictional model is used in the paper and the frictional stress acts as a fraction of the effective stress. Friction heat flux is generated by two contact surfaces interactively, which is distributed the contact surfaces averagely and it is regarded as surface heat flow.

2.1.2. Heat boundary.

It is seen from Fig. 1 that the main heat boundary involves in heat conduction between the rollers and the workpiece, convection and radiation between the workpiece and the surroundings.

$$-k\frac{\partial T}{\partial n}=\left\{\begin{array}{l} h_{con}\left(T-T_R\right) \\ h_\infty\left(T-T_\infty\right)+\sigma_{st}\varepsilon\left(T^4-T_\infty^4\right) \end{array}\quad \left(t>0\right)\right\} \quad (6)$$

where h_{con} shows the interfacial heat transfer coefficient between the roller and the workpiece, and T_R is the temperature of the roller surface. During contact of the steel with the rolls, the workpiece surface is being cooled and conversely the work rolls are gaining heat. Moreover, h_∞ is the heat convection coefficient; T_∞ is the temperature of the surrounding environment; σ_{st} is Stenfan-Boltzmann constant and equals to 5.67×10^{-8} $wm^{-2}K^{-4}$ and ε_r is the surface emissivity and equals to 0-1, which shows the heat radiation boundary condition is nonlinear.

There are high temperature difference between the workpiece surface and core due to heat loss on the workpiece, which makes a great deal of heat flow from the core to the surface through inner heat conduction. Moreover, the heat transfer mechanism is the similar with the heat convection of air cooling in descaling zone. The inner heat conduction and water cooling conduction can be shown the following equations, respectively.

$$\left.\begin{array}{l} k\dfrac{\partial T}{\partial n}+h_w\left(T-T_w\right)=0 \\ k\dfrac{\partial T}{\partial n}+h'_{con}\left(T_s-T_{core}\right)=0 \end{array}\quad \left(t>0\right)\right\} \quad (7)$$

where h_w is the appropriate heat transfer coefficient due to water cooling, T_w is initial water temperature, h'_{con} is heat transfer coefficient of the workpiece, T_s is the temperature of the workpiece surface, and T_{core} is the temperature of the core.

2.1.3. Initial condition and adiabatic boundary.

For the workpiece and the rollers, the initial temperature conditions are given as, respectively.

$$\left.\begin{aligned} T(x,y,z,t) &= T_0 \\ T(r,\theta,z,t) &= T_1 \end{aligned}\right\} \quad (t=0) \tag{8}$$

The boundary conditions of the symmetric center for the workpiece and the roller are written as, respectively.

$$\left.\begin{aligned} \frac{\partial T(t)}{\partial n} &= 0 \quad (x=0, y=0) \\ k\frac{\partial T(t)}{\partial r} &= 0 \quad (r=R) \end{aligned}\right\} \tag{9}$$

where symbol R shows the corresponding radius of the roller.

2.2. Material properties and geometry parameters

The roller material is an iron steel of high chromium and the chemical composition is expressed as Table 1, which shows it is of so many characters like high rigidity, high intensity and high wear resistance. Thus, the rollers can be assumed to be rigid and heat transfer body. The material of the workpiece is a typical carbon steel and its chemical composition is listed in Tables 1 and 2. The material obeys Von Mises yield criterion and Prandtl-Reuss equation. It is assumed that balanced initial temperature distribution occurs in the original workpiece. The workpiece density is 7850 kg/m^3 and the Poisson's ratio is 0.3 the initial temperature of the workpiece is aussumed to be 975°C. The thermo-physical parameters, such as elastic module E, heat dilatation coefficient β, heat conduction rate λ and specific heat c, are the function of temperature.

Table 1

Chemical composition of the roller, %

C	Si	Mn	Cr	Mo	V	W
1.5	0.75	0.67	5.5	2.6	1.43	1.82

Table 2

Chemical composition of the workpiece, %

C	Si	Mn	Cr	Ni	S	P	Cu
0.14	0.27	0.35	0.18	0.21	0.024	0.032	0.23

Three kinds of pass systems are used in the present paper. Namely, they are two ellipse-round rollers, Y type round-flat rollers and Y type arc-flat rollers. The geometric pass systems are shown in Fig. 2.

The research object is a round steel workpiece with 30 mm diameters and 125 mm length, and their material keeps the same for three different pass systems. The 3D finite element model includes 9000 eight-node-hexahedral iso-parametric elements and 9231 nodes. The correlative parameters of three kinds of pass systems are listed in Table 3. The corresponding 3D model is shown in Fig. 3.

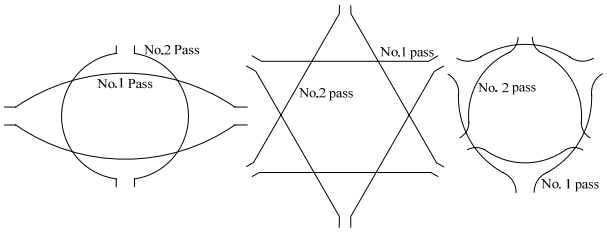

a b c

Fig. 2 Geometric pass, (a) two ellipse-round rollers, (b) Y type three round-flat rollers and (c) Y type three arc-flat rollers

Table 3

Process parameters of the pass systems

	Ellipse-round		Round-flat		Arc-flat	
Reduction, %	41.18	29.89	6.50	7.97	5.13	13.56
Speed, rpm	80.02	102.27	80.02	102.27	80.02	107.91
Gap, mm	2.5	2.5	2.5	2.97	1.8	1.8
Diameter, mm	210	210	210	210	210	210

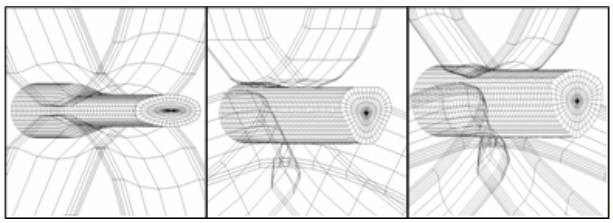

a b c

Fig. 3 3D finite element models, (a) two ellipse-round rollers, (b) Y type round-flat rollers, (c) Y type arc-flat rollers

3. Results and discussion

3.1. Analysis of deformation field

For three different rolling systems, the types of cross section and total effective train are shown in Fig. 4 after the finish of the rolling process. It is seen that the spreads (deformations in the width direction) all occur the gaps between the rollers and mainly are affected by the design of the gaps and the rollers. If the gaps are smaller and the workpiece is away from the roller, it is easier to form the spread. The spread is small due to the constraint effect of the rollers when the workpiece is close to the roller, and the final shape shows overhang in the center of the gaps. By comparing the Y type three flat-passes with two ellipse-round rollers, the spread is smaller in Y type flat-pass because the free spread area decreases. For two ellipse-round rollers, the largest deformation does not occur at the workpiece-roller interface, but lies in the inner position of the workpiece because it is subjected to the radial compression with the reduction rate 41.18%, which shows the deformation has penetrated the core position of the workpiece. For the rolling process of Y type three

round-flat rollers, the deformation of the rolling metal is not penetrated the core position and occurs between the surface and the core because the radial compression is small and the reduction rate only equals to 6.50%. For Y type three arc-flat rollers, due to reduction rate is 5.13%, and the corresponding deformation is not penetrated the core, yet. The flow direction of the rolling metal changes drastically near the free surface of the gaps under the compression effect of arc pass, and it shows the arc edge has influence on the spread. Thus the large shear strain occurs in the gaps where the maximum total effective strain occurs.

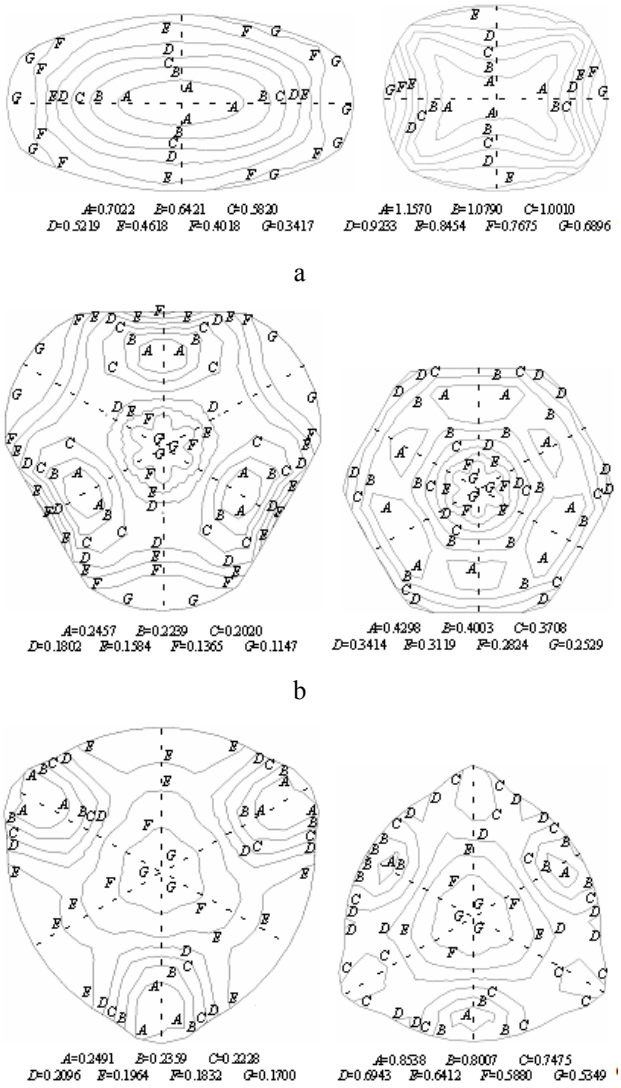

Fig. 4 Total effective strain distribution, (a) two ellipse-round rollers, (b) Y type three round-flat rollers, (c) Y type three arc-flat rollers

3.2. Temperature field

Fig. 5 expresses the temperature distribution on the cross-section when the every pass rolling is complete. It is seen from the figure that the shapes of cross-section show quasicircular, hexagon and peach shape, respectively. The round wire and rod are produced by the two ellipse-round rollers or Y type three arc-flat rollers, which is suitable for the finish rolling pass system. Moreover, the Y type round-flat pass is suitable for the production of triangular or hexagonal wire and it is also used in the extensional pass of other products.

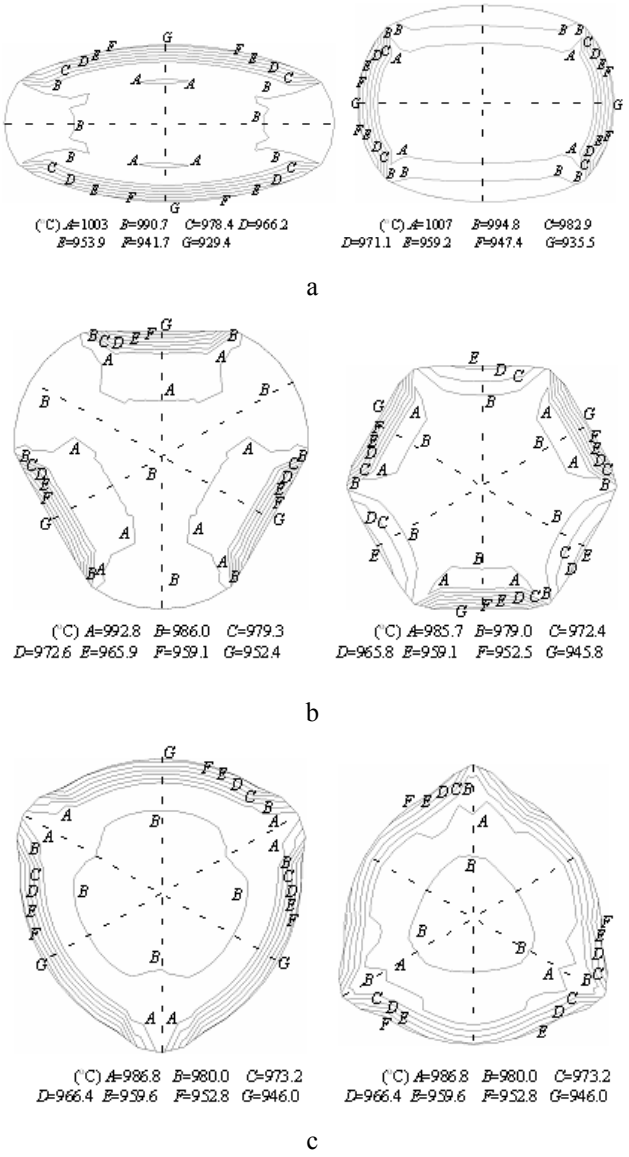

Fig. 5 The distribution of temperature field, (a) two ellipse-round rollers, (b) Y type round-flat rollers, (c) Y type arc-flat rollers

For the rolling of two ellipse-round rollers, a great deal of heat generation due to plastic deformation work and no heat exchange between the core and the surroundings, including the rollers, air and water, which makes the highest temperature occur in the core of the workpiece. Moreover, for the roller surface, especially the contact interface with the roller, because the thermal phenomena, such as heat conduction between the high temperature workpiece and the roller of low temperature, heat convection and radiation between the workpiece and the surrounding environment (air cooling), and forced heat convection with water (water cooling or descaling stage), occurs, and these factors also make the minimum temperature occur at the contact interface. For Y type round-flat pass, it is seen from Fig. 5, b that the highest temperature occurs between the core and the surface of the workpiece. The minimum temperature occurs at the contact interface with the rollers. It can be explained that the largest plastic deformation occurs under the roller and the corresponding

heat generation is more than the other position due to plastic deformation work, moreover, the various heat exchange phenomena appears in the contact area with the roller, which makes the lowest temperature occur at the interface. For the rolling of Y type arc-flat pass, the lowest temperature occurs at the contact interface, and the highest temperature occurs between the core and the surface of the workpiece. It is observed from Fig. 5, c that the area is an approximate ring.

3.3. Force and energy parameters

Fig. 6 shows that the rolling force varies with time. The curves $I_1(II_1)$, $II_1(II_2)$ and $III_1(III_2)$ represent rolling forces of two ellipse-round rollers, Y type three round-flat rollers and Y type arc-flat rollers in the hot rolling of two passes, respectively. It is seen that the rolling force distribution is nonuniform for ellipse-round rollers, and this is explained the reduction rates of the two passes are respective 41.18% and 29.89%. The minimum rolling force differences between the first pass and the second pass occur in the rolling of Y type three round-flat rollers because of the reduction rates of 6.50% and 7.97%, which shows that the reduction rate is dominant for the distribution of rolling force. Namely, rolling forces of three-roller rolling are less than those of two-roller rolling for the same reduction rate. It shows that the design of three rollers makes metal deform uniformly, which results in more steady rolling process. The crack hole and defects of pull and concave caused due to uneven deformation can be eliminated in the rolling of Y type three rollers, which reduces the wear and impact of the rollers. In addition, three rollers can form the closed pass, which makes the length of the roller shorten. Thus, the structure becomes more suitable, and this directly causes the corresponding lateral stiffness of the roller increase and the bending moment decrease. Moreover, there is a very good agreement between the rolling force of two ellipse-round rollers predicted by the simulation and those obtained by experimentation.

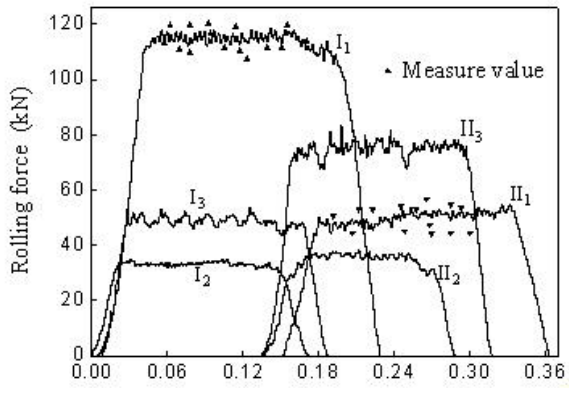

Fig. 6 Rolling force history

3.4. Friction stress

Fig. 7 shows the 3D distribution of the contact frictional stress in the first rolling for three kinds of passes. It is seen from the figure that the friction stress divides into two zones of positive friction stress and negative friction stress. It is observed that the friction stress is positive in backward slip zone and keeps the same with the rolling direction. The area and length of positive friction stress zone are more than those of the negative friction stress, which shows that the friction force is the driving force in hot rolling process of wire. The friction stress is equal to zero on the neutral plane and the friction stress changes its sign. The corresponding negative friction stress occurs in the forward slip, and it shows that the friction force becomes resistance force. Moreover, for two ellipse-round rollers and Y type arc-flat pass, it is observed that the maximum contact frictional stress occurs in the roller entry zone. A variable valley occurs in the middle position along contact width. Namely, the contact friction stress increases locally on both edges of this valley. In addition, for the rolling of Y type round-flat pass, the minimum friction stress occurs on the contact edge, and it can be explained that the reduction rate is small, 6.50%, which does not make metal fill the gaps of the rollers and the spread is also small. Thus the contact width of Y type round-flat pass is smaller than that of the other two rolling modes.

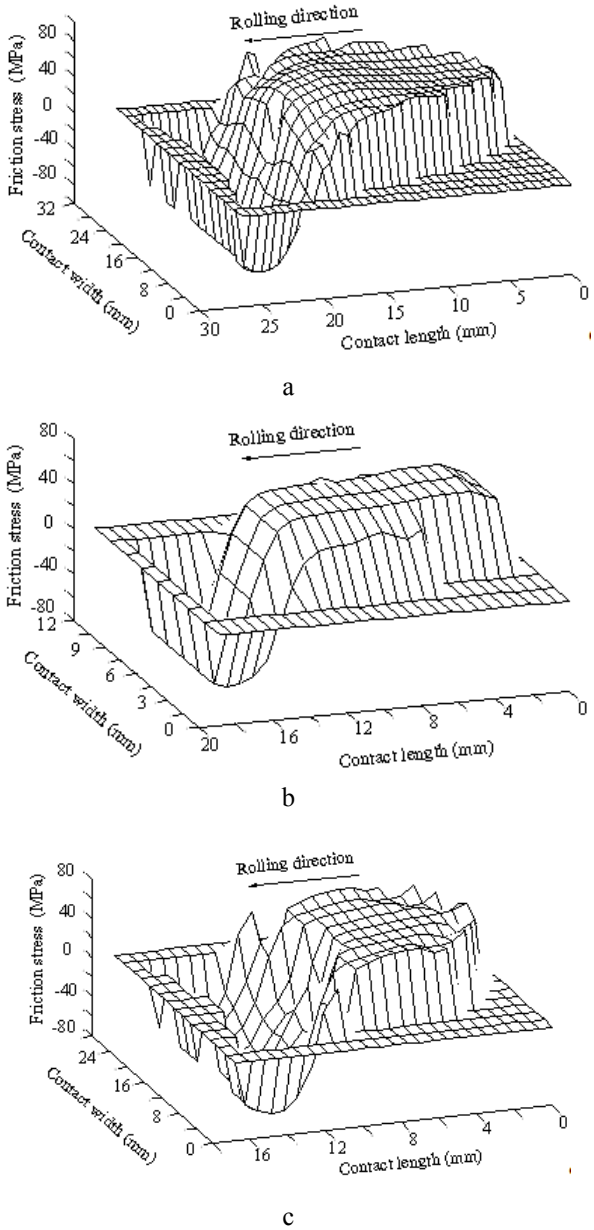

Fig. 7 Friction stress distribution. (a) two ellipse-round rollers, (b) Y type three round-flat rollers, (c) Y type three arc-flat rollers

4. Conclusions

The full three dimensional models based on thermo-mechanical coupling finite element method and updated Lagrangian method have been developed to predict forming mechanism of wire for three different rolling modes. The various thermal exchange phenomena were considered in the paper, including conduction, convection, radiation, force water convection, inner heat conduction, and heat generation due to plastic deformation and friction. The results can indicate as follows.

1. The spread in Y type three round-flat rollers is smaller than that of two-roller rolling. The largest deformation occurs in the inner position of the workpiece because the deformation has penetrated the core position. For the rolling process of three rollers, the metal deformation is not penetrated the core position and the largest strain occurs between the surface and the core.

2. For three different pass systems, the shapes of cross section show quasi-circular, hexagon and peach shape, respectively. The lowest temperature occurs at the contact interface for all rolling systems. In two-roller rolling, the highest temperature occurs in the core, and it appears between the core and the surface for the three-roller rolling.

3. The rolling force distribution of the three-roller rolling is evener than that of the rolling of two rollers. The measured values of rolling forces keep reasonable agreement with the simulation results.

4. For the rolling of two rollers and Y type arc-flat rollers, the maximum contact frictional stress occurs in the roller entry zone. The contact friction stress increases locally on both edges of this valley. For the rolling of Y type round-flat pass, the minimum friction stress occurs on the contact edge without metal filling the gaps of the rollers.

Acknowledgements

The research is supported by National Natural Science Foundation of China and Baosteel Group (51004047, 51075138), Scientific Research Fund of Hunan Provincial Education Department (10B020), Natural Science Foundation of Hunan (09jj4024), Plan Fund of Scientific and Technology of Hunan Province (2009FJ3034), and Provincial Innovative Team of Science and Technology of Hunan (Control of complex networks).

References

1. **Klarin, K.; Mouton, J.P.; Lundberg, S.E.** 1993. Application of computerized slip-line-filed analysis for the calculation of the lever-arm coefficient in hot-rolling mills, J. Mater. Process. Technol. 36(4): 427-446.

2. **Sheikh, H.** 2009. Thermal analysis of hot strip rolling using finite element and upper bound methods, Appl. Math. Modell. 33(5): 2187-2195.

3. **Chung, S.G.; Kuwahara, K.; Richmond, O.** 1993. Streamline-coordinate finite-difference method for hot metal deformations, J. Comput. Phys.,Q. 108(1): 1-7.

4. **Li, Y.G.; Huang, Q.X.; Shen, G.X. et al.,** 2008. Simulation of strip using elastoplastic contact BEM with friction, J. Iron Steel Res. Int. 15(1): 34-38.

5. **Yang, L.C.; Hu, J.X L.; Ning, W. et al.,** 2009. Research on influence of rolling parameters on the rolling process based on numerical simulation, Int. J. Modell., Identi. Control, 7(1): 25-32.

6. **Gudur P.P.; Salunkhe, M.A.; Dixit, U.S.** 2008**.** A theoretical study on the application of asymmetric rolling for the estimation of friction, Int. J. Mech. Sci. 50(2): 315-327.

7. **Liu, X.H.; Shi, X.; Li, S.Q. et al.** 2007. FEM analysis of rolling pressure along strip width in cold rolling process, J. Iron Steel Res., Int. 14(5): 22-26.

8. **Kim, J.; Lee, J.; Hwang, S.M.** 2009. An analytical model for the prediction of strip temperatures in hot strip rolling, Int. J. Heat Mass Transfer 52(7-8): 1864-1874.

9. **Zhang, G.M.; Xiao, H.; Wang**, **C.H.** 2006. Three-dimensional model for strip hot rolling, J. Iron Steel Res. Int. 13(1): 23-26.

10. **Richelsen, A.B.; Tvergaard, V.** 2004. 3D analysis of cold rolling using a constitutive model for interface friction, Int. J. Mech. Sci. 46(5): 653-671.

11. **Du, F.S., Wang, G. G.; Zang, X.L. et al.** 2010. Friction model for strip rolling, J. Iron Steel Res., Int. 17(7): 19-23, 43.

12. **Duan, X.; Sheppard, T.** 2009. Three dimensional thermal mechanical coupled simulation during hot rolling of Aluminium alloy 3003, Int. J. Mech. Sci. 44(10): 2155-2172.

13. **Arif, A.F.M.; Khan, O.; Sheikh. A.K.** 2004. Roll deformation and stress distribution under thermo-mechanical loading in cold rolling, J. Mater. Process. Technol. 147(2): 255-267.

14. **Phaniraj, M.P.; Behera, B.B.; Lahiri, A.K.** 2005. Thermo-mechanical modeling of two phase rolling and microstructure evolution in the hot strip mill Part I. Prediction of rolling loads and finish rolling temperature, J. Mater. Process. Technol. 170(1-2): 323-335.

15. **Serajzadeh, S**. 2008. Effects of rolling parameters on work-roll temperature distribution in the hot rolling of steels, Int. J. Adv. Manuf. Technol. 35(9-10): 859-866.

Licheng Yang, Jingxiang Hu, Liwei Ning, A Romagos

SKIRTINGŲ VIELOS FORMAVIMO BŪDŲ IDENTIFIKAVIMAS TAIKANT JUNGTINĮ TERMOMECHANINĮ METODĄ

R e z i u m ė

Darbe pateikiamas ruošinio ir trijų valcavimo operacijų mechaninis modelis, apimantis du apvalius elipsinius valcus, tris apvalius plokščius Y tipo valcus ir tris lankinius plokščius Y tipo valcus, yra sukurtas naudojant jungtinį termomechaninį tampriai plastinį BEM. Straipsnyje išnagrinėti įvairūs proceso aspektai: laidumas, konvekcija, radiacija, priverstinė vandens konvekcija, vidinis šiluminis laidumas ir šildymas. Skaitinio imitavimo būdu yra tyrinėta skerspjūvio deformacija ir temperatūra, valcavimo jėgos ir erdvinis trinties įtempių pasiskirstymas. Nustatyta, kad ištempimas ir valcavimo jėga yra mažesni Y tipo trijų valcų įtaise, palyginti su dviejų valcų įtaisu, o aukščiausia temperatūra ir didžiausia deformacija atsiranda šerdyje. Valcavimas trimis valcais yra labai tolygus ir sukuria kintamą valcavimo jėgą. Trinties įtempių pasiskirstymas, atliekant trijų valcų operaciją, yra skirtingas. Papildomai buvo imituota dviejų elipsinių apvalių valcų jėgos kitimas, kuris gerai atitiko matavimo rezultatus.

Licheng Yang, Jingxiang Hu, Liwei Ning, A Romagos

SIMULATION OF DIFFERENT FORMING MODE OF WIRE BASED ON THERMO-MECHANICAL COUPLING METHOD

S u m m a r y

In this paper, the mathematic model of workpiece and three rolling passes, including two ellipse-round rollers, Y type three round-flat rollers and Y type three arc-flat rollers, are developed by using thermo-mechanical coupled rigid-plastic FEM. Various thermal transfer phenomena are considered in the paper, such as conduction, convection, radiation, forced water convection, inner heat conduction, and heat generation. Numerical simulations are carried out to examine the strain and temperature on the cross section, rolling force and 3D friction stress distribution. It is found that the spread and rolling force are smaller in Y type three rollers mill than those of two-roller rolling; the highest temperature and the largest deformation all occur in the core for two-roller rolling because the deformation is penetrated the core; the three-rollers rolling is very steady, which makes rolling force more uneven; and the friction stress distribution is different for three-roller rolling systems. In addition, rolling forces history for two ellipse-round rollers are simulated, which provides reasonable agreement with the measured results.

Received March 31, 2011
Accepted December 15, 2011